An integrated approach to quantify the potential local climate mitigation of a district energy network compared to individual air conditioning systems.

G-E Kyriakodis, Emmanuel Bozonnet, Peter Riederer

BS 2021 1-3 SEPT BRUGES
INTERNATIONAL BUILDING PERFORMANCE SIMULATION ASSOCIATION

An integrated approach to quantify the potential local climate mitigation of a district energy network compared to individual air conditioning systems.

G-E Kyriakodis[1,2], Emmanuel Bozonnet[1], Peter Riederer[2]
[1]LaSIE-University of La Rochelle, La Rochelle, France
[2]CSTB, Sophia-Antipolis, France

Abstract

The transition from building to district scale is supported numerically by the nascent field of Urban Building Energy Modelling. However, the concurrent assessment of building energy demand and local climate conditions is sparsely studied explicitly, while there is a lack of integrated tools embedding the modelling of district energy systems. This article presents a developed coupled model to account for building energy needs, urban heat island and site-specific effects, along with the district energy system operation. To illustrate the approach, we examine the mitigation potential of a district network under projected climate conditions for a city with an oceanic climate.

Key Innovations

- Synchronous coupling methodology at urban scale.
- Explicit modelling of urban building stock and local microclimate.

Practical Implications

Thermal assessment of district energy systems combined with microclimate studies.

Introduction

Urban overheating or the so-called Urban Heat Island Phenomenon (UHI) is evident and well documented for hundreds of cities around the world. The intensity of the phenomenon is influenced by the thermal properties of the materials and the urban morphology, which increases the radiative trapping and minimizes the air circulation, including the reduced turbulent transfer in cities. Buildings contribute to the magnitude of urban overheating as they are responsible for the anthropogenic heat emissions due to exfiltration, natural and mechanical ventilation, heat release from HVAC systems as well as convective and radiative heat from the building envelopes.

The impact of the UHI effect has been mainly associated with the deterioration of thermal comfort conditions and the significant increase of the cooling energy demand and the peak electricity consumption (Santamouris, 2020), leading to initiatives towards a zero energy future world through the development of mitigation strategies and action plans.

The transition to zero energy districts treats the urban neighbourhoods as a unity where the modelling accomplishment requires the integration of several challenges. The interconnection of buildings with the local microclimate, the local generation and operation of renewable energy as well as the energy trading concept through the employment of advanced shared energy infrastructures, such as district energy systems, require a holistic methodology for the assessment of their performance (Hong, 2020). To our knowledge there is a lack for simulation platforms that integrate the aforementioned.

In the last years, there is an ongoing rising trend in studies that account for building energy and microclimate concurrently, as shown in Figure 1, instead of treating the urban infrastructures as isolated units. At the same time, the nascent field of urban building energy modelling has arisen to design and operate urban neighbourhoods or districts under multidisciplinary and multiscale approaches.

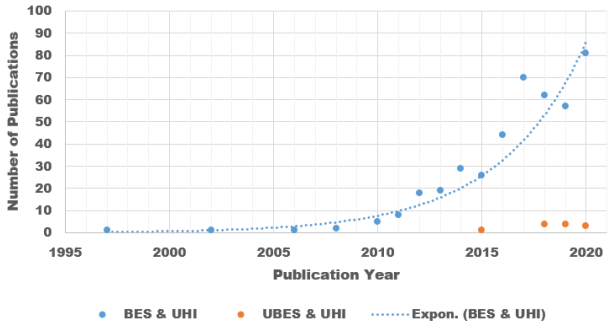

Figure 1: Distribution of Building Energy Simulation studies among articles related to microclimate.

A query on Scopus with the keywords “Building energy simulation” and “urban heat island OR microclimate” shows the increasing trend of this field over the last fifteen years. However, Urban Building Energy Modelling (UBEM) combined with microclimate studies seem still in a germinal stage, given the complexity and the required computing resources.

Several methodologies were developed to capture the impact of urban microclimate on building energy demand, or to quantify the anthropogenic heat contribution from buildings to the outdoor environment (Salamanca, 2011). Most of these approaches, employ either prototype buildings or parametrizations of the outdoor environment (Masson, 2000). Few studies explicitly include building models, but the dynamical interactions are not captured due to the asynchronous link between the simulation

modules, or their spatial and temporal limitations (Palme, 2018).

This study seeks to introduce a new bottom-up methodology for UBEM which operates around four main axes: urban building energy demand, site-specific effects, UHI, and district energy systems, combining a set of tools that serve the spatial scale of urban neighbourhoods under explicit layouts and extended temporal conditions – annual simulations. We conducted a case study of a real neighbourhood in the city of La Rochelle, and we examine the mitigation potential of a district cooling network under projected climate conditions.

Simulation Tools

The study employs a set of simulation tools of different specifications to compensate for mitigating their limitations. The operating spatial scale and the programming language (Python v2.7/v3.6) represent the common characteristics of the tools. This section provides a short description of the selected simulation packages and their key components used to establish the coupled model.

UBEM - DIMOSIM

The UBEM DIMOSIM (Riederer, 2015) is an integrated simulation tool for the analysis of feasibility, conception and operation of district energy system concepts. It consists of (a) building and thermal zone models, (b) thermal and electric network models and (c) a variety of energy system components for the various scales (emitters, hydronic distribution, production, storage and control). It has been developed progressively in CSTB (Center Scientific et Technique du Batiment / Sophia-Antipolis), in the framework of several national and European projects.

The validated thermal zone model corresponds to a rather detailed R-C model (an R31C18 is the default one) to account for the fundamental physical mechanisms occurring at zone level with respect to computational efficiency. The heat transfer mechanisms considered in the thermal zone model are:

- Transient heat conduction through envelopes, roofs and floors as well as internal walls and masses.
- Steady state heat conduction through windows.
- Exterior convective heat exchanges of envelopes, roofs and windows.
- Absorbed shortwave radiation of building envelopes, roofs and windows.
- Longwave radiant heat exchange of envelopes, roofs and window elements taking into account the view factors to sky and ground.
- Interior convective heat exchanges of interior surfaces and windows.
- Radiative gains in the interior surfaces from occupants, equipment and solar radiation.
- Ventilation heat fluxes.
- Thermal bridges.
- The intermediate floors are represented as thermal mass or adjacent envelope between zones (in case of a multi-zone description of the building).

Three types of thermal network models are available in the tool:

1. Steady state model
2. Transient nodal model (one node or multiple nodes)
3. Plug-Flow model

The steady state model is used in this study in which thermal and hydraulic phenomena are considered. In order to calculate the temperature inside the tubes, the thermal losses to the ground are taken into account, depending on tube diameters, thermal insulation, and ground temperature. The tubes are represented by a nodal description where the pressure drop is calculated and the heat from the grid is transferred to the building level substation, represented as heat exchangers.

The boundary conditions of the tool correspond to typical hourly datasets, and the solar radiation model employs hourly data records imported from the meteorological file. It is enhanced with a sky model and simplified mask algorithms at zone or building level.

EnviBatE – site-specific module

EnviBatE (Gros, 2014; Kyriakodis, 2019) stands for environment and buildings. It is a research numerical package conceived to study the interactions between buildings and local microclimate. It is an already coupled model, as it consists of:

- a thermal surface and Reduced-Order (ROM) thermal building models,
- an embedded ROM-CFD (QUIC-urb (Pardyjak, 2003) into a simplified urban canopy model, and
- a sophisticated solar radiation algorithm (SOLENE (Groleau, 2003)).

The latter is responsible for the calculation of the direct and diffuse components as well as the view factors from surface-to-surface and to the sky. It is enhanced with a radiosity algorithm for the estimation of the multi-reflections. These sub-models are finally integrated into a unique zonal model, where buildings and outdoor environment communicate through interfaces, the urban surfaces. The model lacks the representation of latent and natural convection phenomena.

The indoor environment is governed by standard set-point temperatures for the estimation of the energy demand while it lacks the representation of the energy systems.

UWG-UHI

The Urban Weather Generator (Bueno, 2013) is a simplified multi-model based on energy conservation principles capable to estimate the hourly urban canopy air temperature and humidity using weather data from a rural weather station. The model is composed of four modules: a rural station and a vertical diffusion model that allows computing the heat fluxes and the respective vertical profiles at a rural site combined with an urban boundary layer (UBL) model for the estimation of the above-canyon air temperature, and a representative BES-street canyon model to compute the canopy and building energy sensible and latent heat fluxes.

The BES-street canyon models originate from the meso-model approach leading to parameterized schemes of the built environment. It is represented as a ratio of coverage lacking the site-specific characteristics.

Coupled model

In this section we demonstrate the developed synchronous coupling scheme (ping-pong) between the UBEM Dimosim and the microclimate package EnviBatE, as well as the one of their combination with the UWG.

Dimosim-EnviBatE (CM1)

We perform an initial surface-to-surface and zone-to-zone coupling scheme between the tools, by employing the thermal zone model of Dimosim enhanced with the energy systems submodules (generators, emitters, ventilation) to the surface and zonal model of the outdoor environment of EnviBatE.

The tools are bind through the sockets module, allowing the intercommunication between them for extended temporal conditions (annual simulation) and large data exchanges. We developed a specific sub-module responsible for the identification of the exchanged variable and the accurate installation of it inside the matrix systems of the tools.

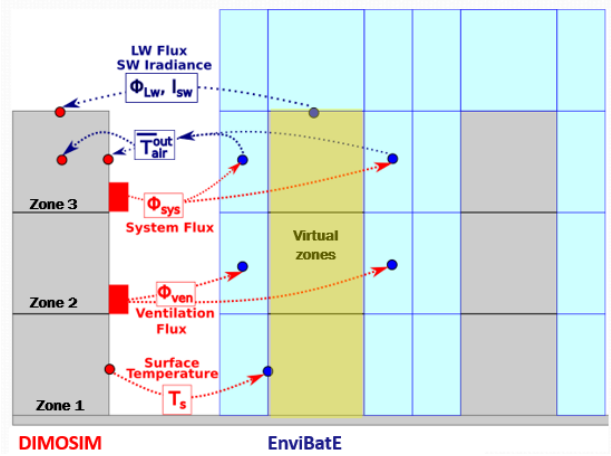

Figure 2: The synchronous coupling scheme between Dimosim and EnviBatE.

More in detail, the thermal zone model of Dimosim calculates the indoor and the envelope temperatures, the ventilation losses and the system rejected heat (in case of local split-units). The aforementioned sensible fluxes are injected in the adjacent canopy air cells of EnviBatE for every thermal zone at each time step of the simulation period. The virtual zones illustrated in Figure *2*, are used to obtain the surface indexation between indoor and outdoor. As a next step the computed outdoor air temperature along with the incident shortwave irradiance and the longwave heat flux of each surface, are set as boundary conditions of the zone model (in Dimosim), as depicted in Figure *2* (for illustration convenience we distinguished the sensible fluxes in several thermal zones). In case of multiple adjacencies, the averaged outdoor air temperature is used while the respective fluxes are weighted based on the corresponding surface ratio.

Dimosim-EnviBatE-UWG (CM2)

Following a similar methodology, we substituted the BES-street canyon model of UWG by the developed refined one. The completion of this task requires the computation of the weighted (in terms of building prototype) mean sensible heat flux emitted from walls, roofs, windows, ventilation, HVAC systems, asphalt roads and concrete sidewalks along with the mean canopy air temperature. These variables are introduced to the UBL model of UWG to calculate the respective air temperature, which is then used as the global boundary temperature of the urban canopy model.

Modeling Workflow

The modelling workflow and the generated individual meshes are presented for the assessment of the thermal performances of an urban neighbourhood in the city of La Rochelle, France.

Study area

The studied area is situated in the Geranium district**,** approximately 2 km away from the city centre, in the north-eastern part of the city of La Rochelle, as shown in Figure 3.

Figure 3: Location of the studied area in La Rochelle, France.

The built area forms a polygon with an approximated surface of 63800m^2. The district borders on the Geraniums cemetery to the West and thus it is unprotected from the dominant western winds and exposed to solar irradiance. The rest of the borders are enclosed by traffic axes. It represents a residential area; as commercial buildings are non-existent according to cadastral data. The outdoor space is composed of asphalt roads and concrete sidewalks, while a small amount of them is sparsely vegetated.

The total number of buildings corresponds to 87, vertically aligned. Every zone is 3m height, giving a total number of 232 thermal zones, as shown in Figure 4a. The maximum building height is 15m, corresponding to building blocks, while the minimum is 3m matching with single-floor detached houses.

The building stock represents a mixture of buildings constructed before the 1970s and newer ones (after the 2000s), as depicted in Figure 4b. The external boundaries are discretised into four layers, representing two plaster layers at the exterior and interior sides, a mass and an insulation layer between them. For the vertical elements indoor insulation is used, while roofs are externally insulated. Figure 5 tabulates and summarizes the envelope

characteristics and the material thermal properties respectively.

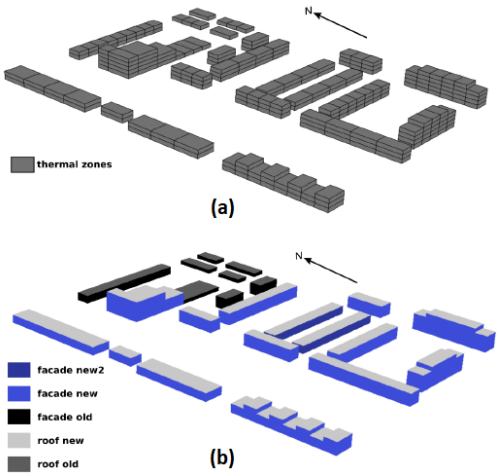

Figure 4: 3-D Visualization of thermal zones (a). Thermal properties attribution of the exterior boundaries (b).

Construction Element	U value [W/m²K]	Thickness [mm]	Albedo [%]
Gfloor old	2.5	10 - 200 - 1.7 - 10	-
Gfloor new	0.4	10 - 200 - 6.4 - 10	-
Roof old	2.08	10 - 4.2 - 200 - 10	26
Roof new	0.33	10 - 8.1 - 200 - 10	20
Wall old	1.59	10 - 200 - 8.6 - 10	30
Wall new	0.36	10 - 200 - 73 - 10	30
Wall new 2	0.36	10 - 200 - 73 - 10	22
Inner mass	1.0	10	-

Figure 5: Thermal & optical properties of surface elements.

The total building envelope area is 37236m², analysed to 23406m² of vertical surfaces and 13830m² of roof and ground floor surfaces. The maximum zone area is 400m² corresponding to single-floor old apartments, while for the building blocks the respective area ranges between 100 and 300m². The glazed area is almost 4681m² resulting in a glazing ratio of 0.2. Interior floors and inner wall mass elements have been kept identical for both building types. Occupancy schedules, internal gains due to appliances and lighting, ventilation/infiltration, and set-point temperatures for each thermal zone are difficult to be gathered at this scale, thus they are set based on the national thermal regulations RT2012.

Weather data

The meteorological data correspond to La Rochelle's typical meteorological year projected to 2050 with CCWorldWeatherGen (Jentsch, 2013) according to the A2 future scenario of forcing agents given in the IPCC Special Report.

This option enables to study the projected cooling energy demand due to the TMY low which corresponds to 179 cooling degree hours (CDH). Table 1, summarizes the maximum, minimum and average dry bulb temperatures, as well as the CDH and HDH for base temperatures equal to 26°C and 19°C for both meteorological files.

Table 1: Input meteorological data.

TMY	CDH	HDH	Dry-bulb temperature [°C]			
			Tmax	Tmin	Taver	
					Cooling	Heating
1995	179	45392	31.9	-5.0	18.8	8.1
2050	350	37636	35.6	-3.1	20.9	9.5

The dominant wind directions are W-NW'n, as given in Figure 6, and W-SW'n for the cooling and heating periods respectively, representing an air circulation from the sea towards the mainland. A future study is planned based on records of the last ten years from the weather station located in La Rochelle airport.

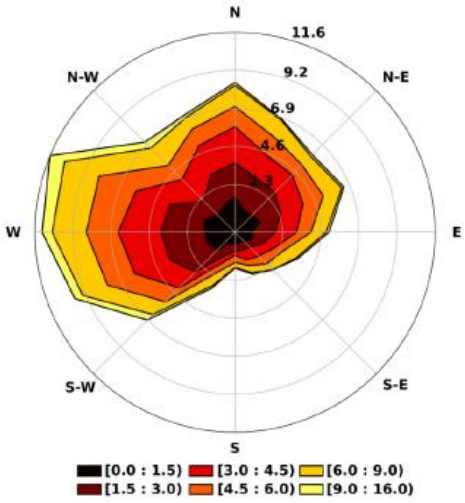

Figure 6: Windrose infilled representation during the cooling period.

Meshes Generation

The generated outdoor zonal mesh has a surface of 207995m². It has been expanded almost four times from the core of the district, mainly in the x-dir (considering north in the y-dir) by 300 m, in order to generate the hypothetical district energy network and the energy hub. It consists of asphalt roads, concrete sidewalks and soil spaces, as shown in Figure 7. Vegetation is taken into account only in solar calculations, considering a monthly constant transmission factor of poplar trees.

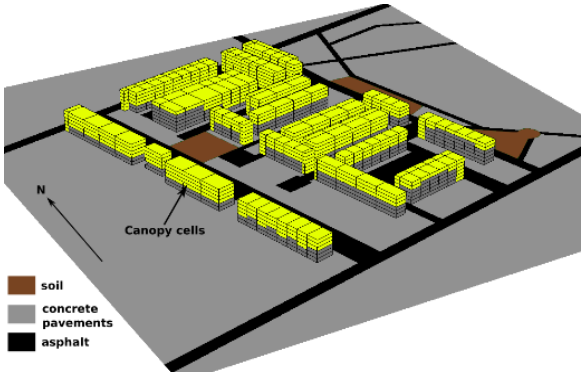

Figure 7: Partly 3-D visualisation of the zonal mesh and the ground surfaces.

https://doi.org/10.26868/25222708.2021.30360

The aforementioned sub-meshes along with the generated solar and airflow grid (presented in the next section) are integrated into a final zonal mesh. The last consists of 5112 air cells divided into 6 horizontal layers. The upper boundary is at 18 m, expanded by one layer (3 m) over the highest building. Each layer consists of 852 air cells, in contact with the ground and the building surfaces. These air cells constitute the urban canopy. The air cells in contact with the thermal zones are forced to have similar dimensions with the adjacent roofs or walls (Figure 7), representing a hexahedral shape (eg: 5m x 10m x 3m). The rest of the canopy cells were meshed based on the Delaunay algorithm given a characteristic length of 10m.

Solar & Airflow pre-calculations

The calculations of solar irradiance have been performed in a fine triangular mesh using SOLENE package. The district is composed of 2197 surfaces. For the generation of the solar mesh, only the solar exposed boundaries were employed, resulting in a total number of 1481 surfaces.

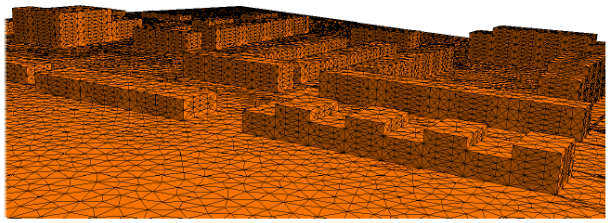

Figure 8: 3-D Visualization of the generated triangulated surface mock-up.

The mesh has been refined by splitting into 16821 triangles, as shown in Figure 8. For building roofs, a characteristic division length of 10 m is preferred, while it is halved to 5 m for the rest of horizontal elements and building walls. This option was chosen for improving computational efficiency due to limited solar shadings at the rooftop.

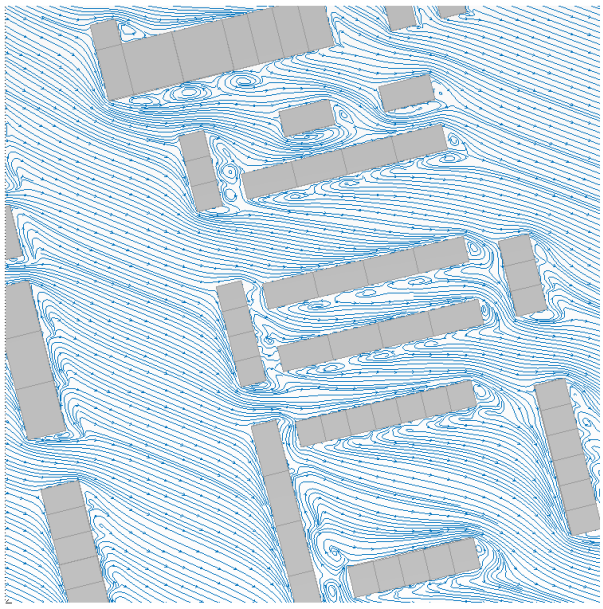

Figure 9: Visualization of streamlines (1.5m) for the dominant W-NW'n wind direction during the cooling period.

The airflow computational mesh is based on a hexahedral staggered grid, composed of cubes of 1(dx) x 1(dy) x 3(dz) m. The final grid domain is set at 457 x 456 x 27 m, at each axis respectively leading to 5.626.584 calculation points. Figure 9 shows the core of the calculation domain and the calculated streamlines for the dominant wind direction during the cooling period.

The calculations have been performed with QUIC-URB for 36 wind directions given a reference value of 3 m/s. In a further step, the extracted outcomes for both wind speed and direction were adapted according to the meteorological data.

Generation of the district network

The network path is generated using the road footprints from the zonal mesh (see: Figure 7), considering the tubes circuit underneath them. The initial network graph is discretized in order to allow the creation of intermediate nodes where the building substations are connected. In parallel, the minimum tube length is calculated, concluding to superfluous node reduction based on the shortest path bridging (spanning tree algorithm) protocol.

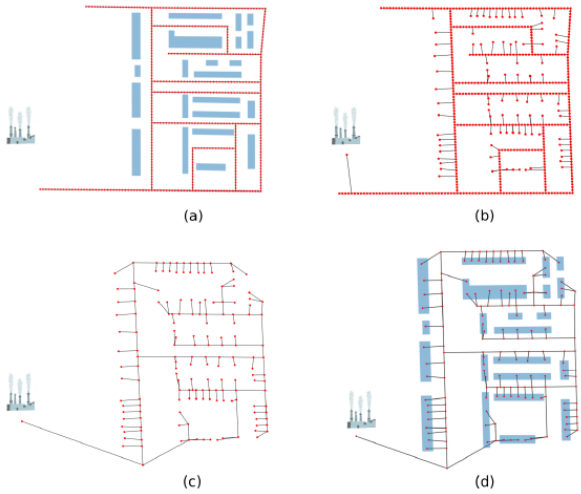

Figure 10: Network generation procedure. Data import (a), node generation (b), superfluous nodes elimination (c), final outcome with building substation-nodes (d).

In addition, each building block has been equipped with a local substation, providing heat to the different thermal zones. The building substations, the calculation nodes, and the optimized network path are depicted in Figure 10d. The piping circuit has a length of approximately 3.5km. The energy hub corresponds to a water-to-water heat pump applied both for cooling and heating period. The nominal heating and cooling supply temperatures have been set to 55ºC and 12ºC for the respective seasons.

Neighbourhood microclimate and energy - results and analysis

The first set of simulation consists of standalone UBEM simulation (Dimosim) for two cooling system scenarios: individual air-conditioners (AC) used in reversible mode, compared to a centralized district energy network (DEN), given the 2050 projected climate as an input. Then,

https://doi.org/10.26868/25222708.2021.30360

depending on the coupling strategy, both scenarios were tested for different boundary conditions:

- the coupled model between Dimosim-EnviBatE (CM1) where the site-specific effects were captured,
- the fully coupled model (CM2) with UWG for the overall UHI effect for the 2050 projected climate.

The aforementioned simulation sets were used to assess and quantify the annual building energy demand (pointing emphasis on the cooling period), as well as to study the mitigation potential of the district energy system implementation. The latter is associated with the elimination of the anthropogenic heat released locally by the AC systems.

Energy assessment

The calculated annual loads are presented in Figure 12 for the cooling (top) and heating period (bottom). As expected, both system scenarios present a significant increase in cooling demand when the UHI effect is considered. More in detail, when the ACs are employed as the cooling providing system, the cooling demand of the neighbourhood increases from 275 MWh to 379MWh, presenting a relative increase of approximately 28% (Figure 12 top-left). The respective outcomes for the DEN scenario exhibit a similar trend, approximating 292MWh in the standalone simulation, while the cooling demand reaches the peak value of 393 MWh under the DEN_UHI (Figure 12 top-right) scenario. However, at this time, the relative increase between the standalone and the UHI scenario is slightly reduced, approximating the value of 26%. This outcome is attributed to the elimination of the rejected heat from the AC systems, and thus the feedback that is stimulated on building energy demand.

A further investigation of the latter is held, by a refinement of the simulation outcomes. The distribution of the cooling demand at the zone level is given in Figure 11, ignoring the ground losses of the piping circuit (Figure 12 top grey and green bars). The plot reveals the slight decrease of the cooling energy demand in the DEN_UHI scenario compared to the AC_UHI accounting for around 5 MWh.

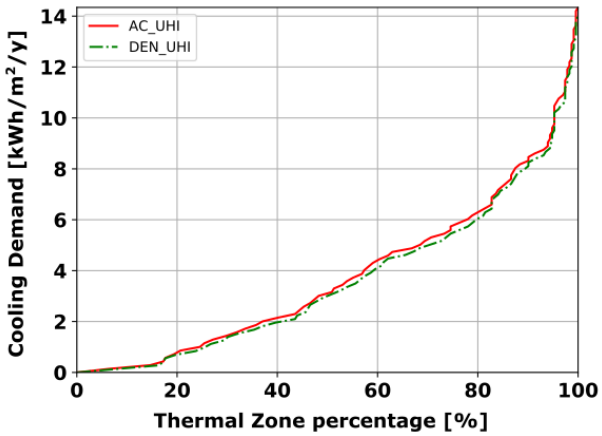

Figure 11:Distribution of cooling demand at the zone level for the AC_UHI (red) and DEN_UHI (green) scenarios.

In the same manner, we define as "cooling penalty" the associated difference of the cooling demand between the DEN (including ground losses) and the AC scenario under the same boundary conditions (standalone and UHI). We observe that the cooling penalty is halved in terms of relative difference, from 6% to 3% when the UHI effect is considered. The latter is essentially attributed to:

- slight decrease of the individual cooling demand at the zone level as the waste heat of the condenser is not considered in the DEN scenario and thus the respective feedback,
- the ground losses present almost a constant value for both simulation scenarios as the ground temperature remains almost identical.

During the heating period, the simulation outcomes present a different behaviour. When the UHI is considered, the heating demand is positively affected and decreases by 4% and 6% for the AC (Figure 12 bottom-left) and DEN (Figure 12 bottom-right) scenario respectively. The site-specific effects, present positive feedback in the DEN scenario, while in the AC one adversely affect the zone demand, due to the cold flux rejected from the evaporators, which locally increases the outdoor air temperature.

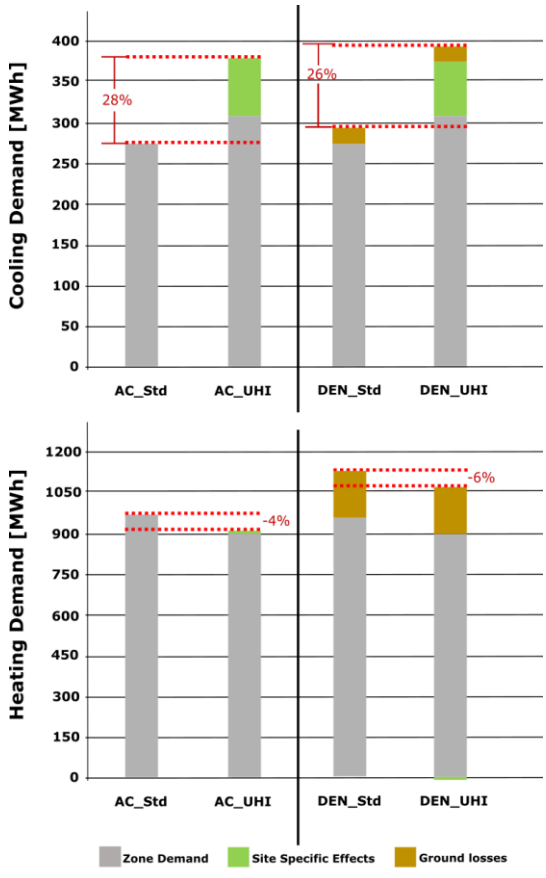

Figure 12: Total cooling (top) and heating (bottom) loads for the DEN and AC scenarios for different boundary conditions.

Microclimate analysis

In order to estimate the mitigation potential of the DEN we computed the Cooling (CDH) and Heating (HDH)

https://doi.org/10.26868/25222708.2021.30360

Degree Hours of the mean canopy air temperature considering as outdoor comfort base temperatures the values of 26ºC and 19ºC for the cooling and heating period respectively. This indicator is widely used in the building energy domain and related to local urban climate modifications.

Table 2: Cooling and heating degree hours for the AC and DEN scenarios extracted with the fully coupled model (CM2).

	2050_UHI	
Scenario	AC	DEN
HDH	35816	35742
CDH	839	765

As shown in Table 2, the CDH of the urban neighbourhood under the UHI simulation scenario increase by 58% compared to the meteorological value (Table 1) when the ACs are considered as the operating energy system while the respective relative increase under the DEN scenario reaches 54%. The reduction of the CDH indicator under the DEN scenario is associated with a mean canopy air temperature reduction over the cooling period of approximately 0.4ºC, which essentially reveals the mitigation capacity of the district energy network. During the heating period, the relative difference is small in both scenarios, approximating 1%.

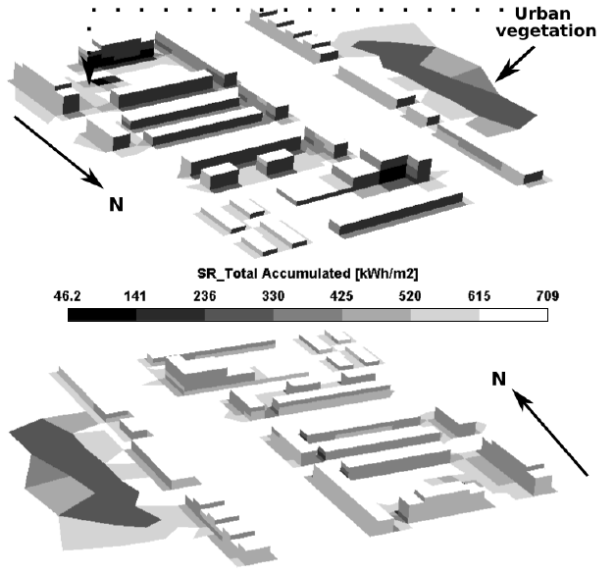

Figure 13: Accumulated incident solar irradiance for the 2050 scenario during the cooling period.

Besides the global microclimate analysis, the developed model accounts for the site-specific effects in order to provide a more detailed thermal inspection of the urban neighbourhood. In Figure 13, we plot the accumulated total incident irradiance of each surface during the cooling period. In the upper part of the figure we plot the building facades facing the north-east direction, while the lower part depicts the south-western oriented ones. The maximum incident solar irradiance is 709 kWh/m^2 found on roofs and horizontal surfaces of the outdoor environment, while the south-western facades receive a heat flux ranging from 615 kWh/m^2 to 709 kWh/m^2. On the contrary, the north oriented facades receive a lower amount of the incident solar irradiance, ranging from 141 kWh/m^2 to 236 kWh/m^2 depending on their height and their specific location inside the district. A small ratio of building surfaces is shadowed by neighbouring obstacles, presenting the lowest amount of incident solar gains ranging between 46.2 kWh/m^2 and 141 kWh/m^2. As highlighted in Figure 12, the urban greenery can reduce solar exposure by almost a factor of three. We must mention that the plotted outputs incorporate also the incident reflected component on every surface. The latter can explain some small differences in adjacent surfaces that are characterized by a different colour scale. This is due to the different view factors of each surface. The detailed solar analysis can act as a first step assessment method of estimating an on-site energy generation potential of PV panels installation, as in (Synnefa, 2017).

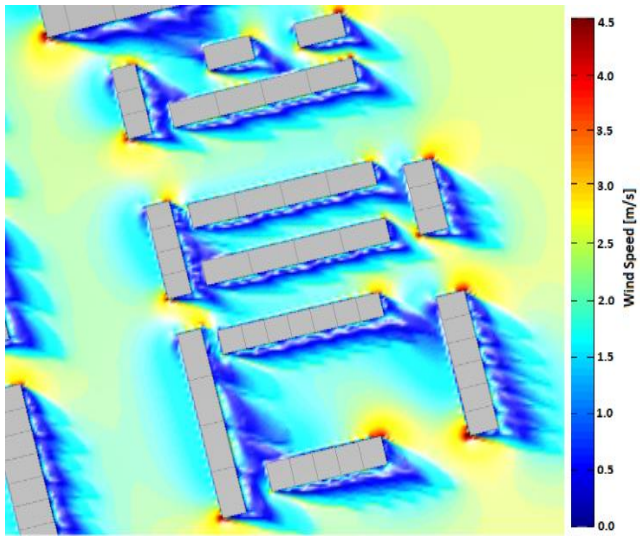

Figure 14: Visualization of wind speed for the dominant wind direction and average wind speed of the meteorological file during the cooling period.

In Figure 14 we plot the wind velocity contour at the pedestrian level for a referenced wind speed (4.2 m/s) and wind direction (292o), complying with the windrose diagram (Figure 6). The selected values represent the average wind speed and dominant wind direction during the entire cooling period. The reduced wind circulation, depicted with blue colour, is characterised by low wind speed values (<1m/s), especially in the lee side of the buildings (the respective streamlines are diluted in Figure 9). This plot combined with Figure 9 and Figure 13 can be used to identify the possible hot spots inside the district.

Conclusions

This paper demonstrates a coupled multi-model to account for urban building energy demand, UHI and site-specific effects as well as the integration of district energy systems to urban energy studies.

The developed methodology is based on a bottom-up approach where the explicit building footprints are enclosed by outdoor air cells of the urban canopy in which heat and mass transfer modelling techniques are

employed under a zonal approach. The derived coupled urban canopy model is linked with a simplified urban boundary module and a vertical diffusion model. The spatial scale of the model corresponds to urban neighbourhoods while the temporal one to annual simulations given the limited execution time (23h/simulation). The model can be used either as a standalone in order to assess the urban thermal performance at various levels, or it can be readily decoupled to support a detailed meso-model.

The neighbourhood case study under future climate conditions for a city with an oceanic climate, examined the mitigation potential of a district energy network as a free on-site heat emitter, compared to individual energy systems, such as AC units, in terms of outdoor thermal comfort and energy efficiency. The simulation outcomes assessed a mitigation capacity of the cooling network close to 2%, considering the CDH as an outdoor thermal comfort indicator related to local climate modifications. The latter is also associated with a mean air temperature reduction of 0.4ºC during the cooling period. However, the mitigation potential of the district energy system is correlated with a cooling penalty due to the ground losses of the tube circuit of approximately 18 MWh which cannot be balanced by the reduction of the cooling demand at the zone level due to the elimination of the rejected heat. Nevertheless, the increased cooling demand when the UHI effect is considered limits the cooling penalty.

Future Developments

The model considers only sensible heat fluxes. Further developments are scheduled in order to account for latent phenomena to include other mitigation strategies such as urban greenery. In parallel, the development of a post-process module is on-going to assess the outdoor thermal comfort, in terms of widely used indices such as UTCI, PET, etc.

Acknowledgement

This study was supported by the European Project PEDOBUR and the Nouvelle-Aquitaine region in the framework of the EQLORE project.

References

Santamouris, M. (2020). Recent progress on urban overheating and heat island research. Integrated assessment of the energy, environmental, vulnerability and health impact. Synergies with the global climate change. *Energy and Buildings*, *207*.

Hong, T., Chen, Y., Luo, X., Luo, N., & Lee, S. H. (2020). Ten questions on urban building energy modeling. *Building and Environment*, *168*, 106508.

Salamanca, F., Martilli, A., Tewari, M., & Chen, F. (2011). A study of the urban boundary layer using different urban parameterizations and high-resolution urban canopy parameters with WRF. *Journal of Applied Meteorology and Climatology*, *50*(5), 1107-1128.

Masson, V. (2000). A physically-based scheme for the urban energy budget in atmospheric models. *Boundary-layer meteorology*, *94*(3), 357-397.

Palme, M. and Salvati, A., "Uwg-trnsys simulation coupling for urban building energy modeling," 2018.

Riederer, P., Partenay, V., Perez, N., Nocito, C., Trigance, R. and T. Guiot (2015). Development of a Simulation Platform for the Evaluation of District Energy System Performances. Proceedings from BS2015: Building Simulation Conference. Hyderabad (India), 7-9 December 2015.

Gros, A., Bozonnet, E. and C. Inard (2014). Cool Materials Impact at District Scale—Coupling Building Energy and Microclimate Models. Sustainable Cities and Society 13, 254–266.

Kyriakodis, G. E., Bozonnet, E., & Riederer, P. (2019, September). Quantifying the Impact of Urban Microclimate in Detailed Urban Building Energy Simulations, Proceedings from BS2019: Building Simulation Conference. Rome (Italy)

Pardyjak, E. and M. Brown (2003). QUIC-URB v1.1 - Theory and User's Guide. California (US)

Groleau, D., Fragnaud, F. and J.-M. Rosant (2003). Simulation of the Radiative Behavior of an Urban Quarter of Marseille with the Solene Model. Proceedings from ICUC-5: Fifth International Conference on Urban Climate. Lodz (Poland), September 2003.

Bueno, B., Norford, L., Hidalgo, J. , and Pigeon, G., "The urban weather generator," Journal of Building Performance Simulation, vol. 6, no. 4, pp. 269–281, 2013.

Jentsch, M. F., James, P. A.B., Bourikas, L. and A. S. Bahaj (2013). Transforming Existing Weather Data for Worldwide Locations to Enable Energy and Building Performance Simulation under Future Climates. Renewable Energy 55, 514–524.

Synnefa, A., Vasilakopoulou, K., Kyriakodis, G. E., Lontorfos, V., De Masi, R. F., Mastrapostoli, E., ... & Santamouris, M. (2017). Minimizing the energy consumption of low income multiple housing using a holistic approach. *Energy and Buildings*, *154*, 55-71.